Rab27a and MyRIP regulate the amount and multimeric state of VWF released from endothelial cells

Thomas D. Nightingale,[1] Krupa Pattni,[1] Alistair N. Hume,[2] Miguel C. Seabra,[2] and Daniel F. Cutler[1]

[1]Medical Research Council Laboratory of Molecular Cell Biology, Cell Biology Unit and Department of Cell and Developmental Biology, University College London, London, United Kingdom; and [2]National Heart and Lung Institute, Imperial College London, London, United Kingdom

Endothelial cells contain cigar-shaped secretory organelles called Weibel-Palade bodies (WPBs) that play a crucial role in both hemostasis and the initiation of inflammation. The major cargo protein of WPBs is von Willebrand factor (VWF). In unstimulated cells, this protein is stored in a highly multimerized state coiled into protein tubules, but after secretagogue stimulation and exocytosis it unfurls, under shear force, as long platelet-binding strings. Small GTPases of the Rab family play a key role in organelle function. Using siRNA depletion in primary endothelial cells, we have identified a role for the WPB-associated Rab27a and its effector MyRIP. Both these proteins are present on only mature WPBs, and this rab/effector complex appears to anchor these WPBs to peripheral actin. Depletion of either the Rab or its effector results in a loss of peripheral WPB localization, and this destabilization is coupled with an increase in both basal and stimulated secretion. The VWF released from Rab27a-depleted cells is less multimerized, and the VWF strings seen under flow are shorter. Our results indicate that this Rab/effector complex controls peripheral distribution and prevents release of incompletely processed WPB content. (*Blood*. 2009;113(20):5010-5018)

Introduction

The endothelial cells that line the blood vascular system play an important role in maintenance of an appropriate inflammatory and hemostatic response.[1,2] One important contribution to this response is exocytosis of specialized rod-shaped storage organelles termed Weibel-Palade bodies (WPBs).[3] These provide a reservoir for the pro-coagulant protein von Willebrand factor (VWF)[4] and other cargo, including the inflammatory cell-surface receptor P-selectin,[5] angiopoietin-2,[6] and interleukin-8[7] (for a complete list, see Metcalf et al[8]).

Both the quantity and structure of secreted VWF are tightly controlled. Low levels or absence of functional VWF in the bloodstream results in von Willebrand disease,[9] the most common inherited bleeding disorder. In addition, the multimeric state of secreted VWF is critical because high-molecular-weight multimers of VWF are the most active with respect to clotting, and loss of this pool alone can result in von Willebrand disease symptoms (type 2A,B),[10] whereas, conversely, excess high-molecular-weight VWF in plasma can result in thrombotic thrombocytopenic purpura, a disease characterized by multiple microvascular occlusions.[11] The release of normal VWF depends on a series of complex biochemical and cell-biologic processes, including the synthesis and processing of VWF itself and its packaging and storage within WPBs, as well as their subsequent exocytosis. Many of these events are poorly understood, especially the way in which the cell biology of WPB formation and function dovetails with the biochemistry of VWF processing.

As VWF is formed in the endoplasmic reticulum, it dimerizes. Subsequent traffic through the Golgi and *trans*-Golgi network (TGN) is accompanied by cleavage of the VWF propeptide, and by initiation of multimerization, which may continue in the WPB after budding from the TGN.[8] Multimerization is crucial for VWF function: at exocytosis VWF is unfurled, by the shear forces present in the vasculature, into long strings that reveal multiple binding sites for platelets and facilitate thrombus formation.[12] Formation of WPB also begins at the TGN where self-association of the propeptide with the D1-D3 domains allows tubulation.[13] These nascent VWF tubules drive the formation of rod-shaped organelles to such an extent that even nonendothelial cells, when transfected with cDNA encoding VWF, can form pseudo-WPBs that recruit appropriate proteins and respond to secretagogue.[14-16] Folding of VWF into WPB tubules is crucial for appropriate release at the cell surface; improper storage results in release of tangled strings.[15]

We and others have shown that WPBs, after they are initially formed, undergo a maturation process that is typified by the acquisition of additional proteins; so far, Rab27a,[17] Rab3D,[18] and CD63[19,20] have been identified. At the same time, WPBs move to a peripheral location within the endothelial cell. More recently, we have shown, using high-pressure freezing and freeze substitution (HPF/FS) followed by electron microscopy (EM), that WPB maturation could be directly visualized. Immature WPBs are electron-lucent and contain tubules that appear disorganized, whereas more mature peripheral WPBs are electron-dense, thinner, and longer with more highly ordered VWF tubules.[21] However, it is unclear how cellular relocation and acquisition of these proteins relate to maturation as visualized by EM, and the role of some of these maturation-specific proteins remains to be characterized. Finally, the critically important functional question remains; how do maturation of WPBs and its control relate to the processing and release of VWF?

Small GTPases of the Rab family play a key role in organelle function, and 2 Rabs, Rab27a (mutation of which leads to Griscelli

Submitted September 25, 2008; accepted February 15, 2009. Prepublished online as *Blood* First Edition paper, March 6, 2009; DOI 10.1182/blood-2008-09-181206.

The online version of this article contains a data supplement.

The publication costs of this article were defrayed in part by page charge payment. Therefore, and solely to indicate this fact, this article is hereby marked "advertisement" in accordance with 18 USC section 1734.

syndrome type II) and Rab3D, have been found localized to WPBs. Overexpression of Rab3D and its dominant negative and constitutively active mutants revealed a negative regulatory role at WPB exocytosis,[18] but the role of Rab27a in WPB function remains elusive. Most Rabs act by interaction with an effector protein,[22,23] but in endothelial cells the appropriate effectors are yet to be characterized for either Rab3D or Rab27a. Here we investigate the role of Rab27a in human umbilical vein endothelial cells (HUVECs) using siRNA-mediated depletion, and we identify an endogenous effector, MyRIP. In addition, we analyzed the physiologic effects of loss of Rab27a and identify how Rab27a is involved in WPB maturation and function.

Methods

Antibodies and immunofluorescence

Rabbit anti-VWF and horseradish peroxidase–conjugated rabbit anti-VWF were purchased from Dako North America (Carpinteria, CA); sheep anti-VWF was from Serotec (Oxford, United Kingdom). Affinity-purified rabbit anti-MyRIP C-terminal antibody was described previously,[24] and goat polyclonal anti-MyRIP antibody was purchased from Abcam (Cambridge, MA). Mouse anti-tubulin antibodies were supplied by Sigma-Aldrich (St Louis, MO). Alexa 488-, 568-, and 680-nm fluorescent conjugates and Alexa 488-nm–conjugated phalloidin were from Invitrogen (Carlsbad, CA).

Immunofluorescence staining was carried out as described previously.[25] Mounted coverslips were imaged at ambient temperature through either a 40× or 63× oil-immersion lens (NA 1.3) on a Leica TCS SPE confocal system (Leica, Wetzlar, Germany) or through a 63× oil-immersion lens (NA 1.4) on a Leica TCS SP5 confocal system. For double- and triple-labeled experiments, the channels were scanned sequentially. Adobe Photoshop CS2 and Illustrator CS2 were used to generate figures from digital images (Adobe, San Jose, CA).

Cell culture and transfection

HUVECs were cultured as described previously.[15] Green fluorescent protein (GFP)–VWF[26] was a gift from J. Voorberg and J. A. Van Mourik (Sanquin Research at CLB, Amsterdam, The Netherlands). GFP-Rab27a[27] and MyRIP-GFP[24] were described previously. Rab27a-mcherry was generated by amplifying mcherry from pCDNA3.1mcherry[28] with primers (GCGCGGTACCGCATGGTGAGCAAGGGCGAG and ATGGACGAGCTGTACAAGGGAGGAATGTCGGATGGAGATTA) and Rab27a from Rab27a-GFP[27] with primers (GCGCGGATCCTCAACAGCCGCATAACCC and ATAATCTCCATCCGACATTCCTCCCTTGTACAGCTCGTCCAT). The 2 products were used as a template for a second round of polymerase chain reaction (PCR) with primers (GCGCGGTACCGCATGGTGAGCAAGGGCGAG and GCGCGGATCCTCAACAGCCGCATAACCC). The resulting product was digested with *Kpn*1 and *Bam*H1 and ligated into a similarly cut vector pCMVMyc,[29] resulting in pCMV-myc-mCherry-Rab27a. DNA (typically 1-5 μg) was transfected into mammalian cells by nucleofection using the program U-001 (Amaxa Biosystems, Gaithersburg, MD).

RNAi and secretion assays

All siRNA duplexes were purchased from QIAGEN (Valencia, CA). The target sequences were: CCAGTGTACTTTACCAATATA-Rab27a(1); CCCATTAGACCTACGAATAAA-Rab27a(2); AAGATAGATGTTCATATTGAA-Rab27a(3); AGAGATCTTAATGGCTATATA-Rab27a(4); AAGGTGGGAATTATTATTTAA-MyRIP(1); CCAAATTTACTTCCCAATAAA-MyRIP(2); nontargeting siRNA sense strand: UGGUUUACAUGUCGACUAA with UU 3′ overhang on both strands.

Cells were transfected with 100 to 200 pmol of targeted or control siRNA by nucleofection (Amaxa Biosystems) using the nucleofection program U-001. Typically, a 15-cm Petri dish with a confluence of 60% to 80% was used for 6 reactions. Reactions were plated into 6-cm Petri dishes and incubated for 2 to 3 days at normal culture conditions. The cells were nucleofected again with 100 to 200 pmol of control or targeted siRNA and plated into 2 wells of a 6-well dish. Two to 3 days later, cells were stained for immunofluorescence, RNA was prepared for quantitative PCR using the QIAGEN RNEasy kit, and a secretion assay and enzyme-linked immunosorbent assay (ELISA) performed.

The VWF secretion assay has been described previously.[25] In short, cells were rinsed and incubated in serum-free medium without secretagogue for 30 minutes. The medium was collected and the cells incubated with serum-free medium containing 100 ng/mL phorbol 12-myristate 13-acetate (PMA; Sigma-Aldrich). The remaining cells were then lysed to determine total VWF levels. Relative amounts of VWF was determined by ELISA[14] and basal and stimulated release presented as a percentage of total VWF present in the cells (basal releasate + stimulated releasate + remainder present in the lysate). Some variation in the size of the releasable pool is apparent in HUVECs because of batch-batch differences in HUVEC stocks and because of differences in confluence (Figure S1, available on the *Blood* website; see the Supplemental Materials link at the top of the online article). This is controlled for using the same batch of HUVECs and plating control and knockdown cells at similar confluence in each experiment. In assays such as the string assay where cells are reseeded, we counted cells and plated them at identical density (see "Flow analysis and quantification of VWE string length").

Microinjection

Cells were nucleofected with siRNA as in "RNAi and secretion assays" and after transfection plated onto scored coverslips. Two days later, 0.1 μg/μL VWF-GFP DNA was injected together with 6.5 μM siRNA into the nuclei of approximately 50 cells over a period of 20 minutes. The next day, coverslips were fixed and stained for immunofluorescence and images acquired with a 63× oil-immersion lens (1.4 NA) on a Leica TCS SP5 confocal system.

Quantitative PCR

Quantitect quantitative PCR primers to Rab27a, MyRIP, rabphilin, Munc13-4, granuphilin, melanophilin, Slp1, Slp2a, Slp3, Slp5, Slac2b, and Noc2 were purchased from QIAGEN. Actin quantitative PCR primers were as follows: GCGAGAAGATGACCCAGAT-actinF; TGGTGGTGAAGCTGTAGCC-actinR. RNA was prepared from knockdown and mock-treated HUVECs using an RNeasy kit (QIAGEN), and cDNA was prepared using the SuperScript III first-strand synthesis system (Invitrogen). DNA was amplified under the following conditions: 95°C, 10 seconds, 56°C, 15 seconds, 72°C, 15 seconds, 40 cycles; amplification was monitored by incorporation of Syber Green (Finnzyme, Espoo, Finland) and analyzed on a Mastercycler ep realplex QPCR machine (Eppendorf North America, New York, NY). Samples were separated on a 2% agarose gel, and single products were verified by melting curve analysis. Quantification was calculated both by the ΔΔCT method[30] and via absolute quantification.

Quantification of WPB distribution

Knockdown and mock-treated cells were plated at a subconfluent density and stained as normal for immunofluorescence and an image acquired at the same plane in each cell. A 40-μm circle was then described around the nucleus and the number of VWF-positive structures present inside and outside the circle determined. Overlapping cells, aberrant cells, and cells in which the perinuclear region touched the cell membrane were excluded. Peripheral and perinuclear WPBs were expressed as a percentage of total WPBs. The distance of individual WPBs from the nucleus was determined using the LASAF software (Leica).

Live cell imaging of WPB movement

Transfected cells expressing Rab27a-mcherry and MyRIP-GFP were imaged through a 63× oil-immersion lens (NA 1.4) on a Leica TCS SP5 confocal system with a heated stage (37°C). The pinhole was opened to 2.513 AU to capture the thickest confocal slice, and images were acquired simultaneously in the red and green channel at 5-second intervals over 5- to

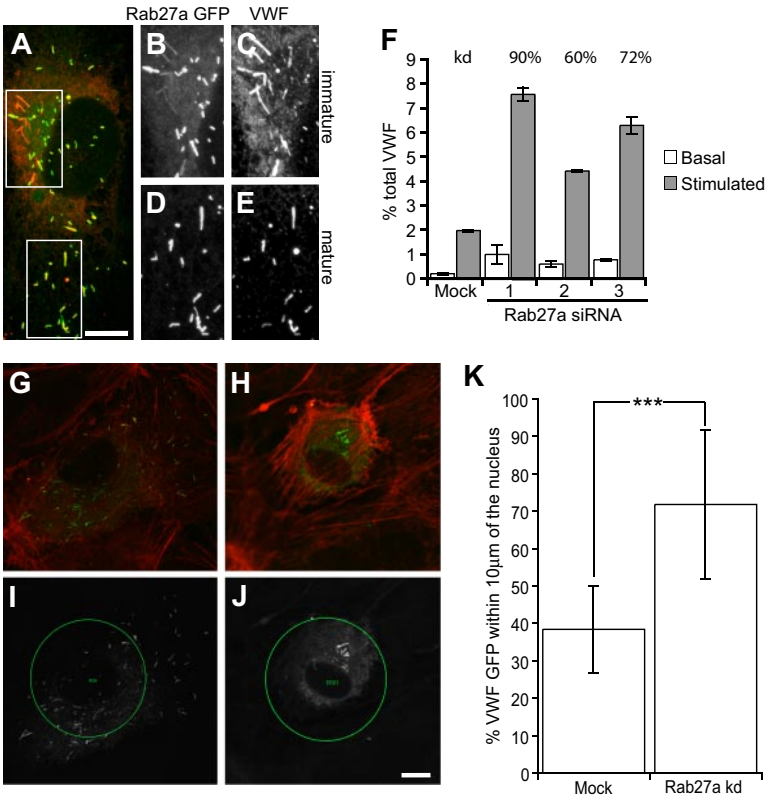

Figure 1. Rab27a-GFP is recruited in a postsynthesis step, and Rab27a knockdown increases stimulus-induced exocytosis of WPBs and results in fewer peripheral WPBs. (A) HUVECs were transfected with Rab27a-GFP and a maximum intensity projection made of confocal images of immunofluorescence staining of VWF (red) and Rab27a-GFP. Boxed images represent magnified images of Rab27a-GFP (B,D) and VWF expression (C,E) in immature (B,C) and more mature WPBs (D,E). (F) HUVECs were treated in 2 consecutive transfection rounds with 3 different siRNA oligonucleotides or a control siRNA oligonucleotide. Cells were incubated with serum-free media for 30 minutes or release media with PMA (100 ng/mL), cells were lysed and the VWF levels of each sample quantified by ELISA. Basal and stimulated release was normalized to total VWF. Rab27a mRNA expression levels in knockdown compared with mock-treated cells as determined by quantitative PCR are above the relevant bars. (G,I) Mock and (H,J) Rab27a siRNA-treated cells were plated out subconfluently after one round of nucleofection and microinjected with siRNA and VWF-GFP. (G,H) Confocal images were acquired of VWF-GFP and rhodamine phalloidin (red). (I,J) A 40-μm circle was placed at the cell nucleus, and the percentage of VWF-positive structures (white) present inside and outside the circle was determined ("Quantification of WPB distribution" in "Methods"). (K) Fifteen mock and 12 knockdown cells were selected from each condition from 2 separate experiments. The percentage present inside the 40-μm circle was plotted. ***$P < .001$ by Student t test and χ^2 test. Bars represent 10 μm. (F,K) Error bars represent SD.

20-minute periods. The image was processed using the LASAF software using a median noise filter with 3 iterations at 3 pixels.

VWF multimer analysis

A total of 1.4% agarose gels were prepared by dissolving Seakem high gelling temperature agarose (Lonza Walkersville, Walkersville, MD) in 0.2 M Tris, 0.1 M glycine, pH 9.0, and sodium dodecyl sulfate (SDS) was added to a final concentration of 0.1%. Basal and secretagogue-stimulated samples from mock- and siRNA-treated cells were concentrated 20-fold using Vivaspin 500 centrifugal filter units (Sartorius, Goettingen, Germany) before loading in a 10 mM Tris, pH 8.0, 1 M ethylenediaminetetraacetic acid, 2% SDS, 8 M urea loading buffer onto the SDS agarose gel. Gels were run at 60 V for 20 minutes and then 36 V for approximately 4 hours in a mini-PROTEAN 3 electrophoresis system (Bio-Rad, Hercules, CA). The separated proteins were transferred to a nitrocellulose membrane and labeled with rabbit anti-VWF antibody (Dako North America) followed by a horseradish peroxidase–conjugated anti–rabbit secondary (The Jackson Laboratory, Bar Harbor, ME) and developed using a Super Signal West Pico chemiluminescent substrate (Pierce Chemical, Rockford, IL). Multimer gels were analyzed using a Molecular Imager GS-800 calibrated densitometer and Quantity One Software (version 4.6.3; Bio-Rad). The global minimum value was subtracted from the trace, and band strength was plotted against distance migrated.

Flow analysis and quantification of VWF string length

Twenty-four hours before experimentation, HUVECs were seeded into μ-slides I (ibidi, Munich, Germany) with a 5-mm-wide channel. The μ-slide was connected to a syringe pump that drew fluid through the chamber at a flow rate giving a wall shear stress of 0.25 Pa (2.5 dyne/cm^2). All perfusions were performed at 37°C; 10 mL PMA (100 ng/mL) was perfused across HUVECs to stimulate VWF release. After PMA stimulation, HUVECs were maintained at 37°C and fixed by perfusion with 20 mL 3% paraformaldehyde (PFA) at a reduced flow rate, and finally left in 3% PFA under static conditions for 20 minutes. PFA was quenched with 50 mM NH_4Cl for 15 minutes at room temperature followed by blocking in PBS, 0.2% gelatin, 0.02% NaN_3. Cells were not permeabilized. Cells were incubated with rabbit anti-VWF (Dako North America) antibody, followed by incubation with an Alexa 568–conjugated anti–rabbit secondary antibody (The Jackson Laboratory). ProLong antifade reagent containing DAPI (Invitrogen) was used as a mounting reagent. Images of labeled VWF strings were obtained by confocal laser scanning microscopy using a Leica TCS SP5 confocal system attached to a Leica DMI6000 microscope (Leica Microsystems). An oil-immersion objective lens 20× (0.7 NA) was used, and imaging parameters were selected to optimize confocal resolution. Images were analyzed using LASAF software to determine the length of individual VWF strings. The number of cells per field was also counted to calculate number of strings per cell. Adobe Photoshop CS2 was used to generate figures from digital images.

Results

Rab27a knockdown increases stimulus-induced WPB exocytosis and changes the cellular distribution of WPBs

The presence of Rab27a on more mature WPB is a well-characterized phenomenon[17] (Figure 1A-E); however, its role in WPB function remains unclear. We used 2 rounds of Rab27a depletion with 3 different siRNA oligonucleotides to investigate the role of Rab27a in the secretion of VWF from primary HUVECs.

SiRNA-mediated depletion with any of the 3 siRNAs typically reduced Rab27a mRNA expression by 60% to 80%, the mean knockdown efficiency in cells exhibiting the phenotype was 71% plus or minus 10.2% (n = 10) as determined by quantitative PCR compared with cells transfected with 2 rounds of control siRNA. Some cell death occurs as a result of nucleofection, and this can affect the confluence of cells. However, no deleterious oligonucleotide transfection-dependent effect was noted on gross morphology or VWF secretion (Figure S2). Rab27a-depleted cells proved hyperresponsive to the secretagogue PMA, with a typical increase

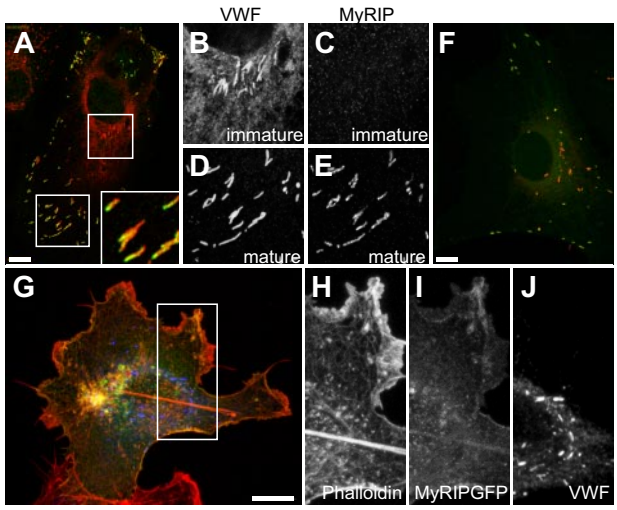

Figure 2. The Rab27a effector MyRIP is present on more mature WPBs. (A) Confocal images acquired of immunofluorescence staining of MyRIP (green), and VWF (red) inset magnified image of polarized localization of MyRIP. Boxed images show magnified images of VWF expression (B,D) and MyRIP (C,E) in immature (B,C) and more mature WPBs (D,E). (F) HUVECs were transfected with MyRIP-GFP, and a maximum intensity projection was made of confocal images acquired of a cell expressing low levels of MyRIP-GFP and VWF (red). (G-J) HUVECs were transfected with MyRIP-GFP, and a maximum intensity projection was made of confocal images acquired of a cell expressing high levels of MyRIP-GFP and VWF (blue) alongside rhodamine-conjugated phalloidin (red). Boxed square shows magnified images of phalloidin (H), MyRIP-GFP (I), and VWF (J). Scale bars represent 10 μm.

in exocytosis of 2-fold over a 30-minute secretion assay, although an increase as high as 3.5-fold was noted (Figure 1F). An increase in basal secretion of approximately 2-fold was also found. A similar increase was also noted using histamine or forskolin as secretagogues (Figure S3). The fold increase positively correlated with the percentage knockdown measured. There was no marked difference in total VWF or in the recruitment of known WPB cargo protein (data not shown). Overexpression of Rab27a-GFP caused a similar increase in stimulated release from HUVECs (Figure S4). This is surprising, as the expected phenotype would be one of suppressed secretion. However, this could represent an indirect effect of sequestering or saturation of Rab-associated cellular machinery.

How does this substantial change in exocytosis relate to the maturation of WPBs? One important aspect of maturation is the movement of WPBs to the cell periphery. Because Rab27a has been associated with organelle movements in a variety of cell types, we determined the effects of Rab27a depletion on WPB distribution. Experiments using first round knockdown of Rab27a by nucleofection followed by microinjection of the siRNA alongside cDNA encoding VWF-GFP (as a marker of injected cells) showed a significant difference in the percentage of peripheral WPBs (Figure 1G-K) with the caveat that the extent of knockdown in individual siRNA-injected cells was impossible to determine. Our data clearly show a role for Rab27a in controlling the release of WPBs and suggest that Rab27a may be involved in peripheral distribution of WPBs.

MyRIP is localized on mature WPBs

Rabs typically act via an interaction with a bound effector,[22,31] and Rab27a has 11 reported effector proteins.[32] To discover which effector(s) are probably functional in endothelial cells, we determined the mRNA expression of the 11 effectors in HUVECs alongside, as controls, the melanocyte cell line MNT-1 and HEK293 cells. RNA and cDNA were made from each line and a 100- to 300-bp fragment of each effector amplified. The fragments were separated on a 2% agarose gel and quantified with respect to an actin standard. As expected, among the highest message levels present in MNT-1 cells was melanophilin, a protein with a well-characterized role in the localization of melanosomes in melanocytes.[33] Of the screened effectors, the most highly expressed in HUVECs was the myosin and Rab27a-interacting protein MyRIP (Figure S5). All the primers were shown to amplify a single product of expected size in at least one of the cell lines tested. As MyRIP was the most highly expressed, we focused on determining its role. We confirmed MyRIP expression in HUVECs by immunofluorescent staining. MyRIP was found, similarly to Rab27a, to be localized on more mature, peripheral WPBs (Figure 2A-E). Interestingly, MyRIP staining was often (but not exclusively) seen to be concentrated at one end of WPBs (Figure 2A large inset). Similarly, overexpressed GFP-tagged MyRIP localized to mature peripheral WPBs at low expression levels (Figure 2F). However, at higher levels of MyRIP expression, it colocalized with phalloidin, indicating that the MyRIP-GFP is now decorating actin structures (Figure 2G-J) and is no longer found on WPBs. This localization/expression pattern of MyRIP suggested that, as for melanosomes in the retinal pigmented epithelium,[24] the protein may serve to anchor WPBs to more peripheral actin structures.

Labeling of actin with fluorescent phalloidin (red or green), alongside MyRIP (Figure 3B) or overexpression of Rab27a GFP (Figure 3A) confirmed that mature WPBs are often found localized with or adjacent to actin structures. In the light of our finding of a polar distribution of MyRIP on WPBs, we also note that a number of WPBs were seen anchored at just one end.

Recruitment of MyRIP to WPBs coincides with a more peripheral distribution

To determine a probable role of a Rab27a/MyRIP complex in endothelial cells, we monitored the recruitment of MyRIP to newly made WPBs. To visualize newly made WPBs, we transfected HUVECs with VWF-GFP, and at hourly time points after transfection, fixed and stained cells for total VWF and MyRIP (Figure 4A). After 4 hours, we began to see newly made WPBs at the TGN, which were negative for MyRIP; at 6 hours, we begin to see more peripheral VWF-GFP and the WPBs at the periphery were positive for MyRIP. By 7 hours, more VWF-GFP-positive structures staining strongly for MyRIP were apparent, and these were present at more peripheral cellular locations. The distance of VWF-GFP-positive WPBs from the nucleus was determined for 5 cells at each

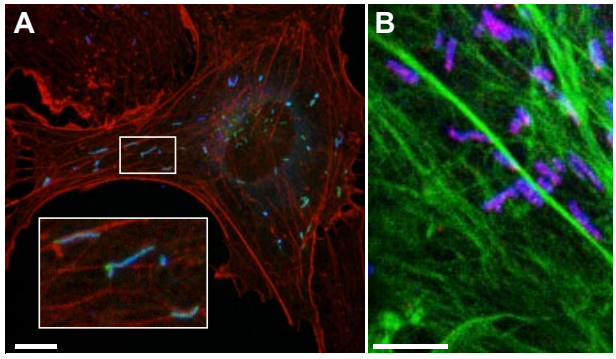

Figure 3. WPBs are often found alongside actin filaments, and some appear to be attached at only one end. (A) HUVECs were transfected with Rab27a-GFP, and a maximum intensity projection was made of confocal images acquired of a cell expressing Rab27a-GFP, VWF (blue), and rhodamine-conjugated phalloidin (red). (B) Maximum intensity projection of confocal images of a HUVECs labeled with MyRIP (red), VWF (blue), and phalloidin Alexa 488 nm (green). Scale bars represent 10 μm.

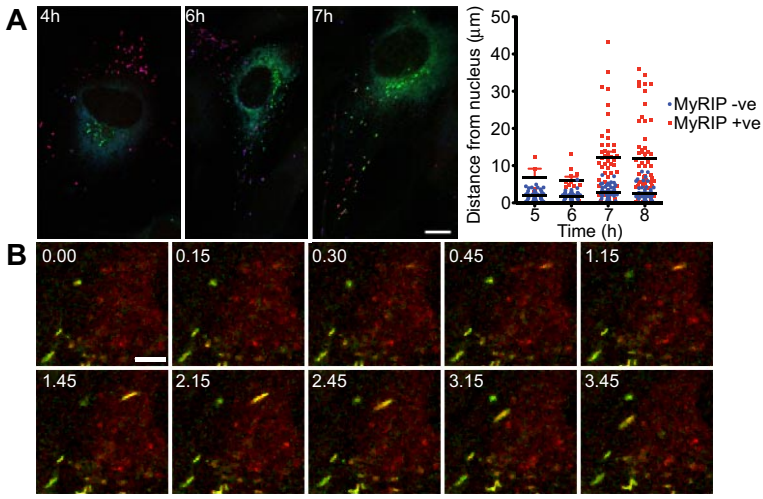

Figure 4. Acquisition of MyRIP expression is coincident with more peripheral WPBs. (A) HUVECs were transfected with VWF-GFP, and cells were fixed and stained for immunofluorescence after 4, 5, 6, 7, and 8 hours. Maximum intensity projection of confocal images was constructed, and expression of MyRIP (red), total VWF (blue), and newly made VWF-GFP was determined (images are shown at 4, 6, and 7 hours). Scale bar represents 10 μm. The distance of VWF-GFP–positive WPBs from the nucleus was determined from 5 cells at each time point and the MyRIP-negative (blue) and MyRIP-positive (red) WPB plotted. Black bars represent the mean distance values; red error bars, SD. (B) Images taken from a 5-minute movie showing the acquisition of Rab27a-mcherry and MyRIP-GFP. Time points are indicated. Scale bar represents 5 μm. Images were acquired on a SP5 confocal microscope with a 2.513A pinhole at one frame every 5 seconds.

time point and the MyRIP-negative and MyRIP-positive WPBs plotted (Figure 4A). All MyRIP-negative WPBs were close to the nucleus, whereas MyRIP-positive WPBs were found farther away.

The recruitment of Rab27a-mcherry and MyRIP-GFP was also monitored in live cells using a confocal microscope with pictures taken every 5 seconds. In images taken from the movie (Figure 4B; Movie S1), we can clearly see a rod-shaped structure that first acquires Rab27a-mcherry followed by MyRIP-GFP and then migrates toward the cell periphery. The initial proximity to the nucleus seen in the movie suggests that it is a newly formed immature WPB, and the fact that the weaker Rab27a-mcherry signal is seen first followed by recruitment of the more brightly labeled MyRIP-GFP suggests that the WPB is not simply moving into the plane of focus. In addition, from immunofluorescence images, we calculated the percentages of WPBs positive for Rab27a and MyRIP (Rab27a-positive, 89.94% ± 6.56%; MyRIP-positive, 73.88% ± 6.32%, n = 8 cells). We noted that all MyRIP-positive WPBs are also positive for Rab27a, whereas a proportion of WPBs exist that are Rab27a-positive but MyRIP-negative. These experiments indicate that Rab27a is acquired first and then goes on to recruit MyRIP and, second, that MyRIP-positive WPBs are associated with a more peripheral distribution.

Knockdown of MyRIP results in increased VWF release and fewer peripheral WPBs

To determine the role of MyRIP in WPB function, we reduced its expression using 2 rounds of transfection with 2 different siRNA oligonucleotides at 2 different concentrations (100-200 pmol). The knockdown efficiency was monitored by SDS–polyacrylamide gel electrophoresis and Western blot (Figure 5A). The knockdown/release data were more variable for MyRIP than for Rab27a, but there is a clear suggestion that HUVECs depleted of MyRIP exhibit an increased release in VWF in a dose-dependent manner (Figure 5B). The increase in release was approximately 2-fold, not as marked as the increase after Rab27a knockdown, suggesting other Rab27a effectors may be involved in regulating exocytosis in addition to MyRIP. After immunofluorescent staining, it was apparent that MyRIP-depleted cells exhibited fewer peripheral WPBs compared with the control (Figure 5C-F). Quantification of this phenomenon ("Quantification of WPB distribution" in "Methods") revealed that the percentage of WPBs within 10 μm of the cell nucleus was significantly increased in MyRIP-depleted cells (Figure 5G). This was similar to the difference in distribution noted for Rab27a-depleted cells (Figure 1) but appears to be more marked perhaps for technical reasons, such as the use of a MyRIP antibody to clearly delineate knockdown versus mock cells or because Rab27a carries out other functions in addition to WPB localization.

Our data suggest that an interaction of Rab27a and MyRIP acts to constrain WPBs at a peripheral localization in the cell. This indicates that MyRIP expression is necessary for normal distribution of WPBs in HUVECs and suggests that a Rab27a/MyRIP complex acts as a negative regulator of WPB exocytosis (although this does not rule out roles for additional Rab27a effectors).

The aberrantly released VWF after Rab27a depletion has a reduced proportion of high-molecular-weight multimers and a higher proportion of low-molecular-weight multimers

We have shown that, during a process of maturation, WPBs acquire Rab27a/MyRIP and that this complex is required for a more peripheral distribution. Our recent EM analysis shows that the VWF tubules change during maturation,[22] and it has long been established that multimerization may occur post-TGN.[34] Does interfering with proteins involved in maturation affect the multimer status of secreted VWF? We analyzed the released VWF from Rab27a-depleted cells to determine whether the multimerization state of the VWF was altered. After multimer analysis of Rab27a-depleted versus control siRNA-treated cells, we noted a difference in the multimer distribution on gels (Figure 6A), which is particularly marked when displayed as a densitometry trace (Figure 6B). There appear to be fewer high-molecular-weight multimers and more lower-molecular-weight multimers in Rab27a-depleted cells compared with mock-treated cells.

VWF strings released after Rab27a depletion are shorter but more numerous than in control cells

Using a flow assay under shear, we analyzed the string length of mock and Rab27a-depleted cells to determine whether the reduction in multimer size also resulted in shorter VWF strings (Figure 7). It was immediately obvious that Rab27a-depleted cells failed to produce the long VWF strings observed in control cells (Figure 7A) but that many more strings were produced (Figure 7A inset graph). We measured the length of individual strings in both Rab27a-depleted and control conditions (Figure 7B,C). We found that the most striking difference in string length was in those less than the 100-μm range (Figure 7C), where the majority of strings produced

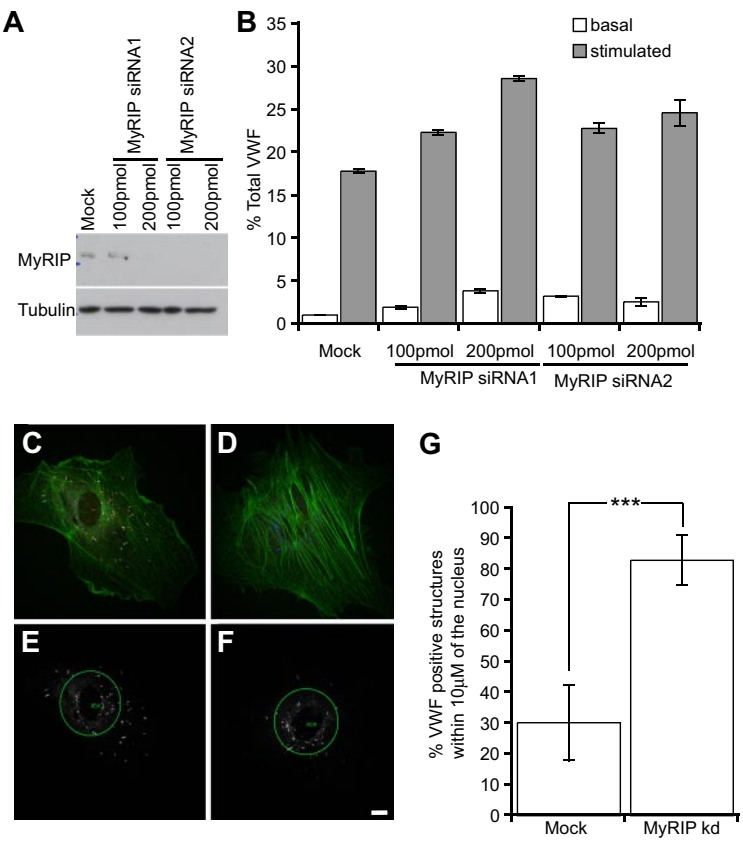

Figure 5. siRNA-mediated knockdown of MyRIP increases stimulus-induced exocytosis of VWF and results in fewer peripheral WPBs. (A) HUVECs were treated in 2 consecutive rounds with 2 different siRNA oligonucleotides (at both 100 and 200 pmol) directed against MyRIP or a control oligonucleotide (at the highest oligonucleotide concentration 200 pmol). Western blot analysis 48 hours after the second round showed down-regulation of MyRIP using a goat anti-MyRIP antibody, whereas tubulin levels were unaffected. (B) Samples of media were acquired after 30 minutes with and without 100 ng/mL PMA, and then cells were lysed and the VWF levels of each sample quantified by ELISA. Basal and stimulated release was normalized to total VWF. (C,E) Mock and (D,F) MyRIP (oligo 1, 200 pmol) and control siRNA-treated cells were plated out subconfluently and visualized by immunofluorescent staining. (C,D) Confocal images were acquired of MyRIP (red), VWF (blue), and actin (green). (E,F) A 40-μm circle was placed at the cell nucleus, and the percentage of VWF-positive structures (white) present inside and outside the circle was determined ("Quantification of WPB distribution" in "Methods"). (F) Scale bar represents 10 μm. (G) Eighteen to 20 cells were randomly selected from each condition from 3 separate experiments. The percentage present inside the 40-μm circle was plotted. ***$P < .001$ by Student t test and χ^2 test. (B,G) Error bars represent SD.

under Rab27a-depleted conditions were significantly shifted toward the lower end of the scale (Figure 7B; Mann-Whitney, $P < .001$). We also noted the formation of some strings with a comparable length to those formed under control conditions (data not shown). These we concluded to be the combined product of several shorter strings. After counting the number of cells per field, we also concluded that a greater number of strings were released in Rab27a-depleted conditions (Figure 7A), consistent with data both from the ELISAs and from the multimer gels and indicating an increase in release of lower-molecular-weight multimers (Figure 6). Taken together, these data demonstrate that, although there is an increase in release of VWF in Rab27a-depleted cells, the released VWF fails to form the longest, most prothrombotic strings compared with those released from control cells but that, in contrast, a greater number of shorter strings are released. Anchoring of WPBs to actin by a Rab27a/MyRIP complex may provide a crucial "brake" to ensure full maturation, thus ensuring that only properly formed VWF is released after secretagogue stimulation.

Discussion

A role for Rab27a in peripheral distribution of organelles has perhaps been best characterized in melanocytes,[27] where a tripartite complex of Rab27a, melanophilin, and MyosinVa is absolutely necessary for the peripheral distribution of melanosomes.[33,35] However, a similar paradigm appears to be true in RPE[24] and PC12 cells[36] where a similar tripartite complex exists, this time using MyRIP and MyosinVIIa or MyosinVa. It now appears that a similar mechanism probably occurs in endothelial cells, whereby MyRIP and Rab27a tether WPBs to actin to support a peripheral localization. In PC12 cells, MyRIP and Rab27a act as negative regulators of exocytosis because overexpression of Rab27a or MyRIP reduces exocytosis.[36] Conversely, in insulin secretion, this complex appears to act as a positive regulator as knockdown of MyRIP or Rab27a reduces release of insulin.[37] Our data are more consistent with published studies on PC12 cells.

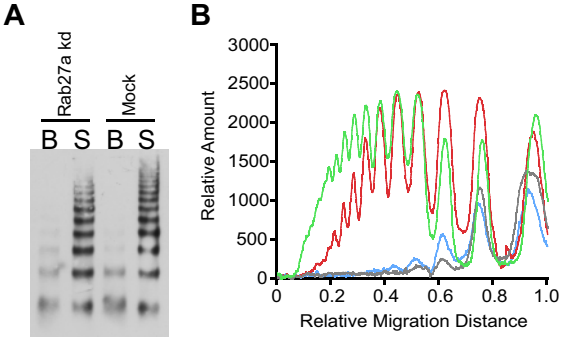

Figure 6. Multimer analysis of Rab27a knockdown and mock-treated HUVECs. (A) HUVECs were treated in 2 consecutive rounds with siRNA oligonucleotides directed against Rab27a or a control oligonucleotide. Samples of serum-free media were acquired after 30 minutes with and without 100 ng/mL PMA. The secreted VWF was concentrated 20-fold and loaded onto a 1.4% agarose multimer gel. The VWF multimer pattern was determined in 3 separate experiments; a representative gel is shown here. (B) Densitometry of multimer gel with the lowest-molecular-weight multimers appearing as peaks to the right of the graph.

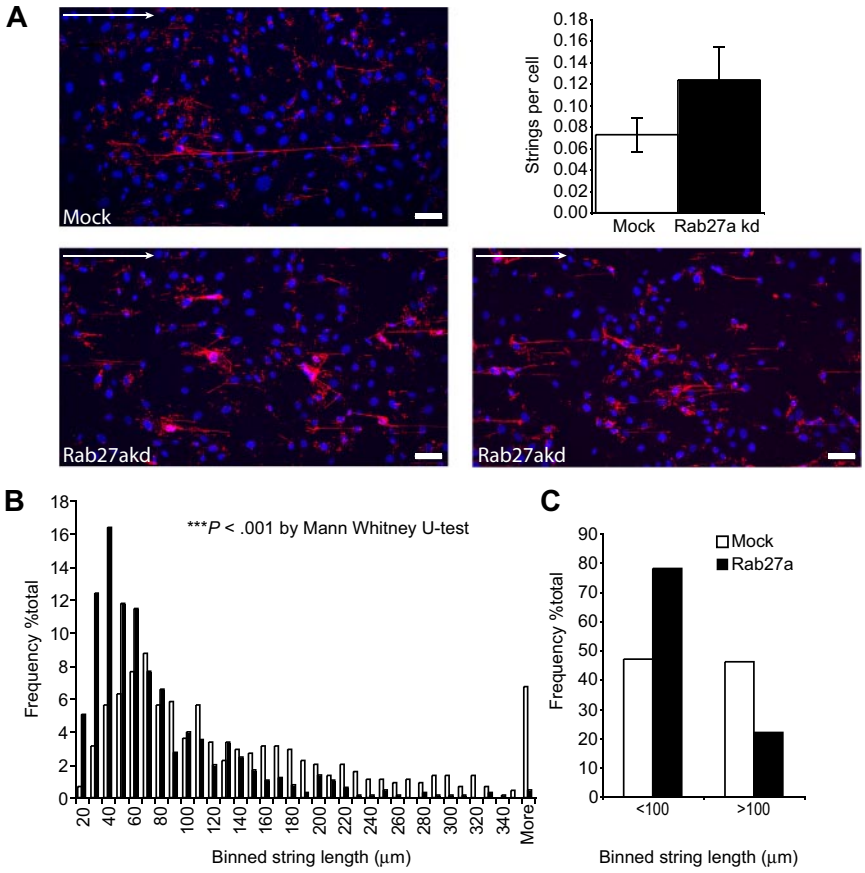

Figure 7. Formation of VWF strings in mock and Rab27a-depleted cells under flow. HUVECs were treated in 2 consecutive rounds with siRNA oligonucleotides directed against Rab27a or a control oligonucleotide, then seeded into μ-slides. HUVECs were stimulated with PMA and fixed under flow ("Flow analysis and quantification of VWF string length" in "Methods"). Fixed VWF strings were labeled with anti-VWF antibodies and imaged by confocal laser scanning microscopy. (A) Representative images of immunolabeled VWF strings released from mock (top panel) and Rab27a-depleted (bottom panels) cells. Arrow represents direction of flow. Bar represents 50 μm. (Inset graph) Number of strings per cell taking into account the number of cells per field of view. Data were collated from at least 5 fields of view taken from 3 separate experiments. Error bars represent SD. (B,C) The length of VWF strings released from either control or Rab27a-depleted cells was measured using LASAF software and binned into 10-μm divisions. Data were collated from at least 5 fields of view taken from 3 separate experiments. (B) Distribution of strings from Rab27a-depleted cells compared with mock-treated cells. Rab27a-depleted cells show a significant increase in shorter strings compared with mock control siRNA-treated cells. $***P < .001$ by Mann-Whitney U test. (C) Distribution of strings more than and less than 100 μm.

The role of the cytoskeleton in WPB function has been studied. Microtubules are required for long-range movement of WPBs from the perinuclear region to the cell periphery, and they may also have a role in exocytosis.[38] Actin has been demonstrated, with certain secretagogues, to be a negative regulatory element in exocytoses,[39] and depolymerization of actin has been shown to increase the rate, distance, and incidence of WPB movement.[38] This is consistent with a negative regulatory role of a Rab27a/MyRIP and actin interaction. We found that cells treated with actin poisons had reduced VWF release and that the increase in VWF release after Rab27a depletion (documented in Figure 1) was similarly reduced by treatment with cytochalasin E (Figure S6). The increase in release seen after Rab27a depletion (Figure 1F) was dependent on microtubules because treatment with nocodazole completely abrogated the observed increase (Figure S7). This argues for a requirement for actin and microtubules in Rab27a function. It remains difficult to determine whether the reduction in exocytosis after treatment was the result of a specific disruption of cortical actin or whether it was the result of a more general actin disruption.

At high levels of expression, MyRIP-GFP decorates actin structures, both stress fibers and what appears to be cortical actin. It is unclear whether this is an attachment via a myosin or a direct interaction. MyRIP has been shown to interact with MyoVIIa in RPE,[24,40] whereas in pancreatic β cells it has been shown to interact with MyoVa.[41] In endothelial cells, no MyoVa was detected by Western blot against the melanocyte-specific isoform (A.N.H., data not shown), but the exact motor involved in WPB function remains to be identified. At high expression levels of MyRIP-GFP, WPBs do not appear to recruit MyRIP and remain in a perinuclear localization. It is possible that the very high ratio of MyRIP to Rab27a causes direct recruitment of Rab27a to actin, inverting the usual chain of events. Certainly, we found expression of high levels of MyRIP-GFP and Rab27a-mcherry together resulted in recruitment of Rab27a to actin (data not shown).

Immunofluorescent localization of MyRIP revealed a markedly polarized distribution on WPBs. The polarization was such that the MyRIP-enriched end of the WPBs was toward the periphery of the cell. It has been suggested that WPBs fuse with the plasma membrane via their ends,[42] and it is possible that Rab27a and MyRIP are involved in this process. We do not see the same polarization of Rab27a-GFP, but this may be an artifact of overexpression. We did note that WPBs are often found in apposition with actin, and we often see WPBs with one end adjacent to the actin filament (Figure 3) as if the WPBs are attached at only one end. Interestingly, MyRIP has also been shown to interact with components of the exocyst[43] and to act as a protein kinase A anchoring protein.[43] This leads to the intriguing possibility that MyRIP is conferring some sort of directionality to WPB either by directly anchoring one end to actin or via an interaction with key exocytic proteins.

There is scope for additional Rab27a effectors playing a role in WPB function, suggested by the fact that ablation of MyRIP gives a weaker phenotype than knockdown of Rab27a alone. We have shown that MyRIP is expressed and has a function in endothelial cells, but other effectors may also be expressed (Figure S5). Certainly in the traffic and exocytosis of other secretory organelles, multiple effectors are involved: for example, in pancreatic β cells MyRIP,[37] granuphilin, Noc2,[44] and Slp5[37] are all expressed and the phenotypes for depletion of granuphilin and MyRIP are markedly different; knockdown of MyRIP reduces release of insulin,[37] whereas knockdown of granuphilin increases release.[45] It is important, therefore, to address the role of each individual effector in

WPB release as some effectors may prove complementary or antagonistic to MyRIP function. An additional complication is that WPBs also recruit Rab3D, and some of the known Rab27a effectors have been demonstrated to also interact with this second Rab.[44,46] It will be important to determine the order of Rab3D/27a recruitment and precisely which Rab recruits which effector. Characterization of MyRIP function is simplified as MyRIP is an effector for only Rab27a,[47] whereas granuphilin and Noc2 have been shown to bind both Rab3D and Rab27a.[44,46] Certainly, the fact that the phenotype is similar to the knockdown of Rab27a suggests that MyRIP is acting via Rab27a. This, coupled with our data implying a sequential acquisition of Rab27a followed by MyRIP, suggests that MyRIP recruitment is dependent on Rab27a and that recruitment is reasonably rapid.

Rab27a has been shown to have a slow rate of guanosine triphosphate (GTP) hydrolysis on granules[48] and a very slow turnover rate from fluorescence recovery after photobleaching experiments,[49] and a similar slow turnover rate has been noted for Rab27a effectors in PC12 cells that include granuphilin and Noc2, whereas other effectors such as Rabphilin have been demonstrated to have a much faster exchange rate.[50] A slow turnover of Rab27a in endothelial cells is consistent with it acting as a scaffold for recruitment of appropriate effectors that change as WPBs mature.

Rab27a appears to provide a brake on exocytosis. Originally, we thought this might be to limit the exocytosis of potentially prothrombotic VWF into the vessel lumen. Analysis of multimerization and of string length in Rab27a-depleted cells suggested that, although more VWF is exocytosed, the amount of high-molecular-weight multimers is reduced, and the string length is shorter (which should therefore make it less prothrombotic). This suggests that the Rab27a may be required to prevent WPBs that are immature (containing incompletely multimerized VWF) from undergoing premature exocytosis.

Specific loss of high-molecular-weight multimers can lead to disease symptoms, so it is possible a bleeding phenotype might ensue. Patients with an absence of Rab27a have Griscelli syndrome type II and a naturally occurring mouse model exists (the ashen mouse). The bleeding phenotype of ashen mice is controversial. The ashen mouse was originally reported to have a bleeding phenotype, but this later proved to be the result of an additional mutation in an orphan nucleotide sugar transporter Slc35d3 resulting in a defect in platelet dense granule function.[51] Maybe an increased release of functionally compromised VWF would cancel out any major differences between WT and ashen mice. This is further complicated when turnover rates of different VWF subpopulations within plasma are taken into account. Certainly, reanalysis of the bleeding phenotype is merited; currently, there are no data of which we are aware describing an aberrant bleeding phenotype in Griscelli type II patients. Altogether, the probable effect of a loss of Rab27a in an in vivo setting is unclear. In vitro we obtained a 2- to 3-fold increase in exocytosis after Rab27a depletion using a number of secretagogues compared with mock-treated cells releasing 2% to 18% of total VWF after stimulation. It is possible that Rab27a and its effectors might play a greater or lesser role under different levels of secretion.

At exocytosis, some signal must release the actin brake. It still remains unclear what triggers this release and how it is modulated. It may be that GTP hydrolysis is required for release but studies to examine this point in exocytosis are complicated by the fact that the GTP locked mutant of Rab27a does not prenylate properly and that injection of nonhydrolysable GTPγS leads to exocytosis,[52] most probably the result of activation of RalA. Identification of the appropriate GAP and the GEF would allow better characterization of the role of Rab27a at exocytosis. The GEF for Rab27a in melanocytes has been identified,[53] and this will provide a good starting point for further characterization.

In conclusion, we have demonstrated that a Rab27a/MyRIP complex is required for peripheral anchoring of WPBs. This anchoring provides a brake on exocytosis and may prevent immature/less multimerized VWF being released. This study also suggests that reanalysis of Griscelli type II patients may reveal the presence of a subtle defect in hemostasis.

Acknowledgments

The authors thank Louise Cramer for helpful discussions and Marie O'Connor for assistance with graphing and statistics.

T.D.N. was supported by the British Heart Foundation (grant PG/O5/062). K.P. and D.F.C. were supported by the Medical Research Council of Great Britain. A.N.H. and M.C.S. were supported by the Wellcome Trust.

Authorship

Contribution: T.D.N. designed, performed, and analyzed research and wrote the paper; K.P. designed, performed, and analyzed research; A.N.H. contributed vital reagents, analyzed data, and wrote the paper; M.C.S analyzed data and wrote the paper; and D.F.C. designed and analyzed research and wrote the paper.

Conflict-of-interest disclosure: The authors declare no competing financial interests.

Correspondence: Daniel F. Cutler, Medical Research Council Laboratory for Molecular Cell Biology, Cell Biology Unit and Department of Cell and Developmental Biology, UCL, Gower St, London WC1E 6BT, United Kingdom; e-mail: d.cutler@ucl.ac.uk.

References

1. Wagner DD, Frenette PS. The vessel wall and its interactions. Blood. 2008;111:5271-5281.
2. Wakefield TW, Myers DD, Henke PK. Mechanisms of venous thrombosis and resolution. Arterioscler Thromb Vasc Biol. 2008;28:387-391.
3. Weibel ER, Palade GE. New cytoplasmic components in arterial endothelia. J Cell Biol. 1964;23:101-112.
4. Wagner DD, Olmsted JB, Marder VJ. Immunolocalization of von Willebrand protein in Weibel-Palade bodies of human endothelial cells. J Cell Biol. 1982;95:355-360.
5. Bonfanti R, Furie BC, Furie B, Wagner DD. PADGEM (GMP140) is a component of Weibel-Palade bodies of human endothelial cells. Blood. 1989;73:1109-1112.
6. Fiedler U, Scharpfenecker M, Koidl S, et al. The Tie-2 ligand angiopoietin-2 is stored in and rapidly released upon stimulation from endothelial cell Weibel-Palade bodies. Blood. 2004;103:4150-4156.
7. Wolff B, Burns AR, Middleton J, Rot A. Endothelial cell "memory" of inflammatory stimulation: human venular endothelial cells store interleukin 8 in Weibel-Palade bodies. J Exp Med. 1998;188:1757-1762.
8. Metcalf DJ, Nightingale TD, Zenner HL, Lui-Roberts WW, Cutler DF. Formation and function of Weibel-Palade bodies. J Cell Sci. 2008;121:19-27.
9. Ruggeri ZM. von Willebrand factor: looking back and looking forward. Thromb Haemost. 2007;98:55-62.
10. Federici AB, Mannucci PM. Management of inherited von Willebrand disease in 2007. Ann Med. 2007;39:346-358.
11. Sadler JE. von Willebrand factor, ADAMTS13, and thrombotic thrombocytopenic purpura. Blood. 2008;112:11-18.
12. Dong JF, Moake JL, Nolasco L, et al. ADAMTS-13 rapidly cleaves newly secreted ultralarge von Willebrand factor multimers on the endothelial surface under flowing conditions. Blood. 2002;100:4033-4039.

13. Huang RH, Wang Y, Roth R, et al. Assembly of Weibel-Palade body-like tubules from N-terminal domains of von Willebrand factor. Proc Natl Acad Sci U S A. 2008;105:482-487.
14. Blagoveshchenskaya AD, Hannah MJ, Allen S, Cutler DF. Selective and signal-dependent recruitment of membrane proteins to secretory granules formed by heterologously expressed von Willebrand factor. Mol Biol Cell. 2002;13: 1582-1593.
15. Michaux G, Abbitt KB, Collinson LM, Haberichter SL, Norman KE, Cutler DF. The physiological function of von Willebrand's factor depends on its tubular storage in endothelial Weibel-Palade bodies. Dev Cell. 2006;10:223-232.
16. Wagner DD, Saffaripour S, Bonfanti R, et al. Induction of specific storage organelles by von Willebrand factor propolypeptide. Cell. 1991;64:403-413.
17. Hannah MJ, Hume AN, Arribas M, et al. Weibel-Palade bodies recruit Rab27 by a content-driven, maturation-dependent mechanism that is independent of cell type. J Cell Sci. 2003;116:3939-3948.
18. Knop M, Aareskjold E, Bode G, Gerke V. Rab3D and annexin A2 play a role in regulated secretion of vWF, but not tPA, from endothelial cells. EMBO J. 2004;23:2982-2992.
19. Harrison-Lavoie KJ, Michaux G, Hewlett L, et al. P-selectin and CD63 use different mechanisms for delivery to Weibel-Palade bodies. Traffic. 2006;7:647-662.
20. Vischer UM, Wagner DD. CD63 is a component of Weibel-Palade bodies of human endothelial cells. Blood. 1993;82:1184-1191.
21. Zenner HL, Collinson LM, Michaux G, Cutler DF. High-pressure freezing provides insights into Weibel-Palade body biogenesis. J Cell Sci. 2007; 120:2117-2125.
22. Grosshans BL, Ortiz D, Novick P. Rabs and their effectors: achieving specificity in membrane traffic. Proc Natl Acad Sci U S A. 2006;103:11821-11827.
23. Jordens I, Marsman M, Kuijl C, Neefjes J. Rab proteins, connecting transport and vesicle fusion. Traffic. 2005;6:1070-1077.
24. Lopes VS, Ramalho JS, Owen DM, et al. The ternary Rab27a-Myrip-Myosin VIIa complex regulates melanosome motility in the retinal pigment epithelium. Traffic. 2007;8:486-499.
25. Lui-Roberts WW, Collinson LM, Hewlett LJ, Michaux G, Cutler DF. An AP-1/clathrin coat plays a novel and essential role in forming the Weibel-Palade bodies of endothelial cells. J Cell Biol. 2005;170:627-636.
26. Romani de Wit T, Rondaij MG, Hordijk PL, Voorberg J, van Mourik JA. Real-time imaging of the dynamics and secretory behavior of Weibel-Palade bodies. Arterioscler Thromb Vasc Biol. 2003;23:755-761.
27. Hume AN, Collinson LM, Rapak A, Gomes AQ, Hopkins CR, Seabra MC. Rab27a regulates the peripheral distribution of melanosomes in melanocytes. J Cell Biol. 2001;152:795-808.
28. Shu X, Shaner NC, Yarbrough CA, Tsien RY, Remington SJ. Novel chromophores and buried charges control color in mFruits. Biochemistry. 2006;45:9639-9647.
29. Strom M, Hume AN, Tarafder AK, Barkagianni E, Seabra MC. A family of Rab27-binding proteins: melanophilin links Rab27a and myosin Va function in melanosome transport. J Biol Chem. 2002; 277:25423-25430.
30. Livak KJ, Schmittgen TD. Analysis of relative gene expression data using real-time quantitative PCR and the 2(-Delta Delta C(T)) method. Methods. 2001;25:402-408.
31. Novick P, Medkova M, Dong G, Hutagalung A, Reinisch K, Grosshans B. Interactions between Rabs, tethers, SNAREs and their regulators in exocytosis. Biochem Soc Trans. 2006;34:683-686.
32. Fukuda M. Versatile role of Rab27 in membrane trafficking: focus on the Rab27 effector families. J Biochem. 2005;137:9-16.
33. Hume AN, Ushakov DS, Tarafder AK, Ferenczi MA, Seabra MC. Rab27a and MyoVa are the primary Mlph interactors regulating melanosome transport in melanocytes. J Cell Sci. 2007;120: 3111-3122.
34. Wagner DD, Marder VJ. Biosynthesis of von Willebrand protein by human endothelial cells: processing steps and their intracellular localization. J Cell Biol. 1984;99:2123-2130.
35. Hume AN, Tarafder AK, Ramalho JS, Sviderskaya EV, Seabra MC. A coiled-coil domain of melanophilin is essential for myosin Va recruitment and melanosome transport in melanocytes. Mol Biol Cell. 2006;17:4720-4735.
36. Desnos C, Schonn JS, Huet S, et al. Rab27A and its effector MyRIP link secretory granules to F-actin and control their motion towards release sites. J Cell Biol. 2003;163:559-570.
37. Waselle L, Coppola T, Fukuda M, et al. Involvement of the Rab27 binding protein Slac2c/MyRIP in insulin exocytosis. Mol Biol Cell. 2003;14:4103-4113.
38. Manneville JB, Etienne-Manneville S, Skehel P, Carter T, Ogden D, Ferenczi M. Interaction of the actin cytoskeleton with microtubules regulates secretory organelle movement near the plasma membrane in human endothelial cells. J Cell Sci. 2003;116:3927-3938.
39. Vischer UM, Barth H, Wollheim CB. Regulated von Willebrand factor secretion is associated with agonist-specific patterns of cytoskeletal remodeling in cultured endothelial cells. Arterioscler Thromb Vasc Biol. 2000;20:883-891.
40. El-Amraoui A, Schonn JS, Kussel-Andermann P, et al. MyRIP, a novel Rab effector, enables myosin VIIa recruitment to retinal melanosomes. EMBO Rep. 2002;3:463-470.
41. Ivarsson R, Jing X, Waselle L, Regazzi R, Renstrom E. Myosin 5a controls insulin granule recruitment during late-phase secretion. Traffic. 2005;6:1027-1035.
42. Romani de Wit T, de Leeuw HP, Rondaij MG, et al. von Willebrand factor targets IL-8 to Weibel-Palade bodies in an endothelial cell line. Exp Cell Res. 2003;286:67-74.
43. Goehring AS, Pedroja BS, Hinke SA, Langeberg LK, Scott JD. MyRIP anchors protein kinase A to the exocyst complex. J Biol Chem. 2007;282: 33155-33167.
44. Matsumoto M, Miki T, Shibasaki T, et al. Noc2 is essential in normal regulation of exocytosis in endocrine and exocrine cells. Proc Natl Acad Sci U S A. 2004;101:8313-8318.
45. Kasai K, Fujita T, Gomi H, Izumi T. Docking is not a prerequisite but a temporal constraint for fusion of secretory granules. Traffic. 2008;9:1191-1203.
46. Kuroda TS, Fukuda M, Ariga H, Mikoshiba K. The Slp homology domain of synaptotagmin-like proteins 1-4 and Slac2 functions as a novel Rab27A binding domain. J Biol Chem. 2002;277:9212-9218.
47. Fukuda M, Kuroda TS. Slac2-c (synaptotagmin-like protein homologue lacking C2 domains-c), a novel linker protein that interacts with Rab27, myosin Va/VIIa, and actin. J Biol Chem. 2002; 277:43096-43103.
48. Kondo H, Shirakawa R, Higashi T, et al. Constitutive GDP/GTP exchange and secretion-dependent GTP hydrolysis activity for Rab27 in platelets. J Biol Chem. 2006;281:28657-28665.
49. Handley MT, Haynes LP, Burgoyne RD. Differential dynamics of Rab3A and Rab27A on secretory granules. J Cell Sci. 2007;120:973-984.
50. Handley MT, Burgoyne RD. The Rab27 effector rabphilin, unlike granuphilin and Noc2, rapidly exchanges between secretory granules and cytosol in PC12 cells. Biochem Biophys Res Commun. 2008;373:275-281.
51. Chintala S, Tan J, Gautam R, et al. The Slc35d3 gene, encoding an orphan nucleotide sugar transporter, regulates platelet-dense granules. Blood. 2007;109:1533-1540.
52. Fayos BE, Wattenberg BW. Regulated exocytosis in vascular endothelial cells can be triggered by intracellular guanine nucleotides and requires a hydrophobic, thiol-sensitive component: studies of regulated von Willebrand factor secretion from digitonin permeabilized endothelial cells. Endothelium. 1997;5:339-350.
53. Figueiredo AC, Wasmeier C, Tarafder AK, Ramalho JS, Baron RA, Seabra MC. Rab3GEP is the nonredundant guanine nucleotide exchange factor for Rab27a in melanocytes. J Biol Chem. 2008;283:23209-23216.